Coexistence of superconductivity and magnetism in the composite material $(La_{1.85}Sr_{0.15}CuO_4)_{1-x}(La_{0.3}Dy_{0.4}Sr_{0.3}MnO_3)_x$

Daniel Hsu,[1,2] T. Geetha Kumary,[1,*] L. Lin,[3] and J. G. Lin[1,4,†]
[1]*Center for Condensed Matter Sciences, National Taiwan University, Taipei 106, Taiwan*
[2]*Department of Mechanical Engineering, National Taiwan University, Taipei 106, Taiwan*
[3]*Department of Physics, National Changhua University of Education, Changhua 500, Taiwan*
[4]*Center for Nanostorage Research, National Taiwan University, Taipei 106, Taiwan*
(Received 23 February 2006; revised manuscript received 21 October 2006; published 6 December 2006)

The electrical and magnetic properties of the composites $(La_{1.85}Sr_{0.15}CuO_4)_{1-x}(La_{0.3}Dy_{0.4}Sr_{0.3}MnO_3)_x$ with $0 \leqslant x \leqslant 0.15$ were studied by resistivity, ac susceptibility, and magnetization measurements. The undoped $La_{1.85}Sr_{0.15}CuO_4$ (LSCO) undergoes a superconducting transition at ~40 K, whereas $La_{0.3}Dy_{0.4}Sr_{0.3}MnO_3$ (LDSMO) exhibits an insulator-to-metal transition (T_{MI}) ~ 100 K and a spin glass transition (T_f) ~ 70 K. The saturation magnetization of the composites shows an increase with increase in x. The onset temperature (T_c) of the superconducting transition of LSCO remains almost unaltered upon intercalation with LDSMO, whereas the superconducting volume fraction decreases drastically with increase in x. The normal state resistivity of LSCO changes from the initial metallic behavior to that of an insulator when x is increased. The signature of another magnetic transition is observed in the composites below T_f in the ac susceptibility and magnetization measurements. The nature and frequency dependence of this magnetic transition could not, however, be determined due to the onset of superconducting transition. On the basis of analysis of the resistivity data, it is conjectured that intercalation of LSCO with LDSMO leads to charge localization in LSCO which suggests possible microscopic phase separation of LSCO into hole-rich and hole-poor regions.

DOI: 10.1103/PhysRevB.74.214504 PACS number(s): 74.72.Dn, 74.62.Dh, 74.25.Fy, 74.25.Ha

I. INTRODUCTION

Transition metal oxides with perovskite structure have generated a great deal of interest since the 1950s due to the variety of electrical and magnetic properties that they exhibit. Two important findings in this context are the occurrence of high temperature superconductivity (HTSC) in hole doped copper oxide perovskites, and colossal magnetoresistance (CMR) in manganates. The undoped parent compounds of the cuprate superconductors are insulators and they exhibit long range antiferromagnetic order due to the ordering of Cu^{2+} moments.[1,2] The antiferromagnetic order disappears upon hole doping and superconductivity sets in above a critical doping level. The complex phase diagram of the seemingly simple copper oxide superconductor $La_{1-x}Sr_xCuO_4$ has been extensively studied and the magnetic state is found to change dramatically[3–12] with Sr doping. From muon spin rotation and nuclear magnetic resonance measurements,[13–17] the superconducting order is observed to coexist with the spin glass order in $La_{1-x}Sr_xCuO_4$ until a critical doping $x_c = 0.19$, where the normal state pseudogap closes. An increase in the spin-glass ordering temperature is also reported with Fe doping[18] in $La_{2-x}Sr_xCu_{1-y}Fe_yO_4$ in the underdoped regime. The suppression of superconductivity by magnetic order has also been studied extensively in manganite oxide ferromagnet/cuprate superconductor heterostructures recently, due to its importance in understanding the mechanism of HTSC.[19–21]

In this paper we report the results of our investigations carried out on the composites $(La_{1.85}Sr_{0.15}CuO_4)_{1-x}(La_{0.3}Dy_{0.4}Sr_{0.3}MnO_3)_x$. The study of variation in physical properties of the cuprate superconductor $La_{1.85}Sr_{0.15}CuO_4$ (LSCO) for small intercalations of the CMR material $La_{0.3}Dy_{0.4}Sr_{0.3}MnO_3$ (LDSMO) was taken up in view of the similarity in the crystal structure and composition of the cuprate superconductors with those of the CMR manganates.[22] LDSMO was chosen in this study due to its low ferromagnetic coupling compared to $La_{0.7}Sr_{0.3}MnO_3$ and also due to the fact that it undergoes a spin glass transition[23,24] below ~70 K. It is felt that studies on the composites can reveal the effect of short range magnetism on high temperature superconductivity. One can think of several, different possibilities for the effect of magnetism of LDSMO on the physical properties of LSCO. First of all, considering the fact that superconducting LSCO is a doped antiferromagnet, it is possible that the short range antiferromagnetism in LDSMO could enhance the superconductivity of LSCO. Second, the proximity of a material like LDSMO may result in magnetic pair breaking in LSCO causing a partial quenching of superconductivity. Third, the short range magnetic ordering in LDSMO can induce a spin glass ordering in LSCO at a higher temperature than that of the undoped LSCO which is ~45 mK.[15] Hence it is necessary to carry out experimental investigations on the composites to get clear knowledge on the effect of proximity of LDSMO on the physical properties of LSCO.

II. SAMPLE PREPARATION AND CHARACTERIZATION

A series of samples $(La_{1.85}Sr_{0.15}CuO_4)_{1-x}(La_{0.3}Dy_{0.4}Sr_{0.3}MnO_3)_x$, denoted as $(LSCO)_{1-x}(LDSMO)_x$, with $x=0$, 0.015, 0.03, 0.06, 0.09, 0.12, 0.15, and 1 were prepared by the solid state reaction route. Polycrystalline samples of LSCO were prepared by heat treating stoichiometric quantities of high purity La_2O_3,

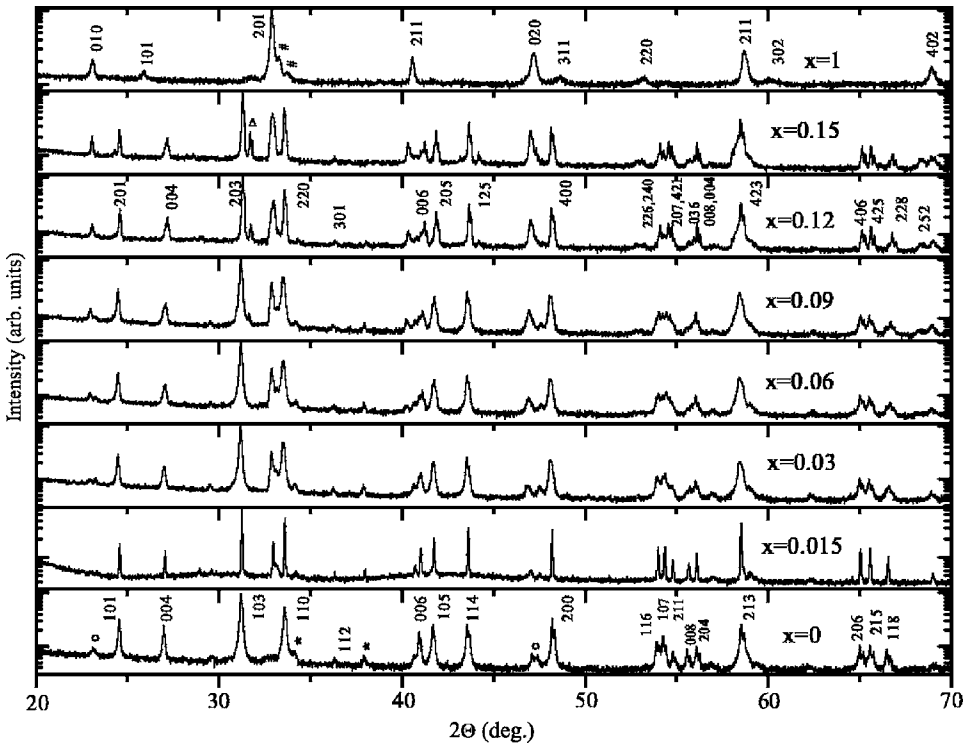

FIG. 1. XRD patterns of LSCO ($x=0$), LDSMO ($x=1$), and the composites. Intensities are plotted on a logarithmic scale.

SrO, and CuO powders at 1050 °C for 36 h in oxygen atmosphere. The heat treatment was repeated three times after grinding and repelletizing each time to ensure the homogeneity of the samples. Similarly, polycrystalline LDSMO was prepared by the solid state reaction of La_2O_3, SrO, Dy_2O_3, and Mn_3O_4. The raw materials were mixed and pelletized and were sintered at 1000 °C for 15 h, 1400 °C for 10 h and 1400 °C for 8 h with intermediate grinding and repelletizing. The samples were finally quenched at LN_2 temperature from 1000 °C. The required amounts of LSCO and LDSMO were mixed, ground, and pressed into pellets and an additional heat treatment at 1000 °C for 48 h was given in oxygen atmosphere to prepare the composites.

The crystal structure and the phase purity of all the samples were determined by analyzing the x-ray diffraction pattern (XRD). The XRD measurements were carried out using Cu $K\alpha$ radiation with the PANalytical; X' Pert PRO diffractometer. Figure 1 represents the x-ray diffraction patterns of all the samples that are studied. The intensities are plotted on a logarithmic scale for ensuring clarity of the low intensity lines. A very small quantity of $(SrCu)_{3-\delta}O_{3-\delta}$ (*) is present as an impurity in LSCO. There are another two lines with very small intensities, marked by "∘," which could not be indexed to any known phases. We believe them to be some compound of La, since the other impurity lines correspond to Sr and Cu rich phases. A small amount of $DyMnO_3$ (♯) is present in LDSMO. Until $x=0.09$, all the prominent peaks in the XRD patterns of the composites could be indexed to those of LSCO and LDSMO. The remaining lines with very low intensities correspond to the impurity phases present in the undoped LSCO and LDSMO used for making the composites. The impurity phases, which are seen in LSCO and LDSMO, are absent in the composites with $x=0.12$ and 0.15. Instead, a new impurity line is seen in these composites. We attribute this line to $(La,Sr)(La,Dy)_2CuO_4$, which, we believe, arises due to the reaction between the impurities present in the undoped compounds, since they disappear in the composites with $x=0.12$ and 0.15. Thus we find that chemical reactions have not taken place between LSCO and LDSMO in the composites.

The XRD pattern of the undoped LSCO can be indexed to a tetragonal unit cell with lattice parameters $a=3.779\,56(24)$ Å and $c=13.2451(8)$ Å and that of LDSMO to an orthorhombic unit cell with lattice parameters $a=7.734(5)$ Å, $b=3.8511(15)$ Å, and $c=3.839(3)$ Å. A broadening is observed in some of the lines in the XRD pattern of LSCO in the composites, especially in (110) and (200) lines, with increase in x until $x=0.12$. For the composites with $x=0.12$ and 0.15 the structure changes to orthorhombic with a doubling of the lattice parameters along a and b. These results suggest that there is a distortion in the LSCO lattice upon intercalation with LDSMO. The variation in lattice parameters with x is shown in Fig. 2(a). There is an overall increase in the a lattice parameter except for $x=0.015$ whereas the c lattice parameter shows a decrease with increase in x. This leads to a decrease in the c/a ratio which is shown in Fig. 2(b). The c/a ratio is observed to decrease rapidly with increase in x for low values of x and shows a tendency for saturation when x is increased beyond 0.06. The lattice parameters (a/b, $b/2$, and c) of the composites with $x=0.12$ and 0.15 are plotted on the right y-axis. (The dotted lines in the figure are just guides to the eyes.)

Scanning electron micrographs (SEM) of all the samples were taken in order to obtain an idea about the distribution of LDSMO in LSCO. The SEM of undoped LSCO and the composite with $x=0.03$ are shown in Figs. 3(a) and 3(b), respectively. LSCO is observed to form grains with an average size of the order of a few microns. The La-to-Sr ratio in

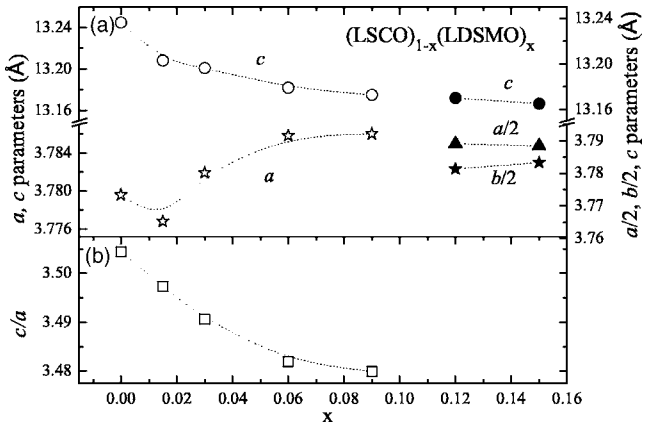

FIG. 2. (a) Variation in the lattice parameters of LSCO with x. Lattice parameters a and c for composites with $x=0$ to 0.09 are plotted on the left y-axis and $a/2$, $b/2$, and c for the higher values of x in the right y-axis. (b) The variation in c/a ratio with x. The dotted lines are guides to the eyes.

LSCO is determined to be around 1.850:0.144 from EDAX measurements which is very close to the stoichiometry (1.85:0.15) of LSCO that is taken for the present study. The second phase corresponding to LDSMO is observed in the SEM pictures of the composites. Small particles of LDSMO (size of the order of a few hundreds of nanometer) are observed to be distributed over the LSCO matrix without any preferential adherence to the grain boundaries. The density of these small particles increases with increase in x. The SEM of the composites taken after slicing them also showed a similar distribution of the fine grains of LDSMO over the larger grains of LSCO indicating the homogeneous distribution of LDSMO in the composites.

The electrical properties were studied by resistivity measurements using the typical four probe method. Silver paint was used to make electrical contacts on the sample and Cu wires were used as electrical leads. The magnetic properties were studied by ac susceptibility and dc magnetization measurements using a physical property measurement system (PPMS, Quantum Design).

III. RESULTS AND DISCUSSION

The temperature dependence of resistivity and ac susceptibility for LDSMO are shown in Fig. 4. As seen from the resistivity data, when the temperature is lowered, LDSMO undergoes an insulator-to-metal transition around 100 K. A spin glass transition is also observed at a lower temperature $T_f \cong 70$ K, which is manifested as a cusp in ac susceptibility data. The results of the detailed studies carried out on the spin glass transition of LDSMO are published elsewhere.[23] The magnetization (M), measured as a function of the applied field (H) at 10 K is shown in the inset of Fig. 4. The saturation magnetization is observed to be more than 100 emu/g.

The variation of resistivity of the undoped LSCO as well as the composites is plotted as a function of temperature in Fig. 5. The undoped LSCO shows a temperature dependence

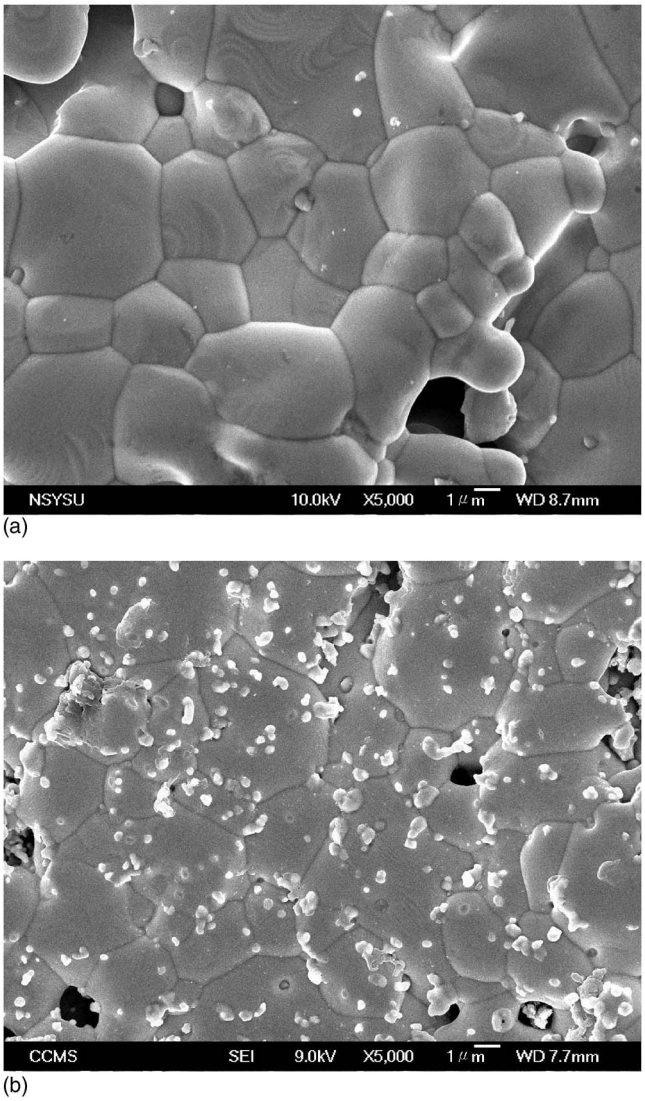

FIG. 3. SEM of (a) LSCO and (b) the composite with $x=0.03$.

of resistivity that is typical of a metal whereas the composites with $x \geq 0.03$ show semiconductinglike behavior. The composite with $x=0.015$ shows a metallic behavior down to ~80 K, below which a semiconductinglike upturn is observed in the resistivity. It is seen that the composites with $x \geq 0.03$ show almost similar temperature dependence of resistivity. The values of the resistivity of the composites with $0.03 \leq x \leq 0.12$ are comparable to each other. They all have a resistivity of the order of 0.05 Ω cm at 25 K. Hence the resistivity data shown in Fig. 5 are multiplied by 1.5, 3, 3.5, and 3 for $x=0.06$, 0.09, 0.12, and 0.15, respectively, for the clarity of presentation. The composite with $x=0.15$ has a slightly higher value of resistivity, around 0.1 Ω cm at 25 K. The onset temperature of the superconducting transition (T_c) of undoped LSCO is measured to be around 40 K indicating that the Sr doping is optimum in this compound. It can also be inferred from the sharpness of the superconducting transition that the sample is highly homogeneous. The region near the superconducting transition of LSCO is expanded and is shown in the inset of Fig. 5 for $x=0$ and 0.015.

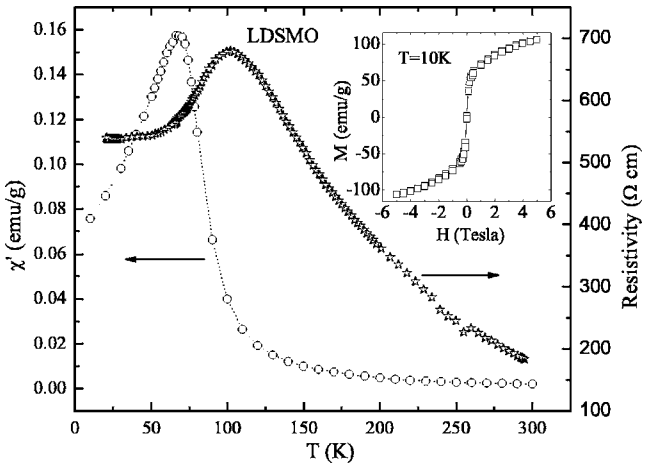

FIG. 4. ac susceptibility (circles) and resistivity (stars) of LDSMO as a function of temperature. The variation of magnetization as a function of applied field, at 10 K, is shown in the inset.

As can be seen from Fig. 5, the resistivity of the composites is larger than that of the undoped LSCO for all the samples that we have studied. Except for the one with $x=0.015$ all the other composites show an increase in room temperature resistivity of about one order of magnitude greater than that of the undoped LSCO. Even in the case of the sample with $x=0.015$, where the LDSMO content is only 1.5% there is a substantial increase ($\sim$50% at room temperature) in resistivity compared to the undoped LSCO and semiconducting up turn in resistivity below $\sim$80 K. The observed semiconducting like behavior (for $x \geqslant 0.03$) and the large increase in resistivity of the composites is quite surprising because the major phase in the composites is LSCO, which is metallic. The SEM pictures do not show any selective deposition of LDSMO in the grain boundaries of LSCO. So, the semiconductinglike behavior cannot be attributed to grain boundary effects. Also, the onset T_c does not vary much among the composites, but there is a broadening in the superconducting transitions in the composites as compared to that of the undoped LSCO. ΔT_c $[T_c(\text{onset}) - T_c(R=0)]$ for the undoped LSCO is around 2 K whereas it is more than 4 K in the composites. It is to be noted here that the resistivity does not vanish completely in the superconducting state for the composites even for the smallest value of x pointing out the fact that there is a drastic reduction in the superconducting volume fraction of LSCO on intercalation with LDSMO. From the results of XRD and SEM, we do not expect that there is any chemical reaction between the composites which may lead to such drastic reduction in the superconducting volume fraction and the change in resistivity behavior. Also, we think that if there is a chemical reaction between the composites there should have been a reduction in T_c. These facts suggest that something should be happening at the microscopic level in LSCO upon intercalation with LDSMO.

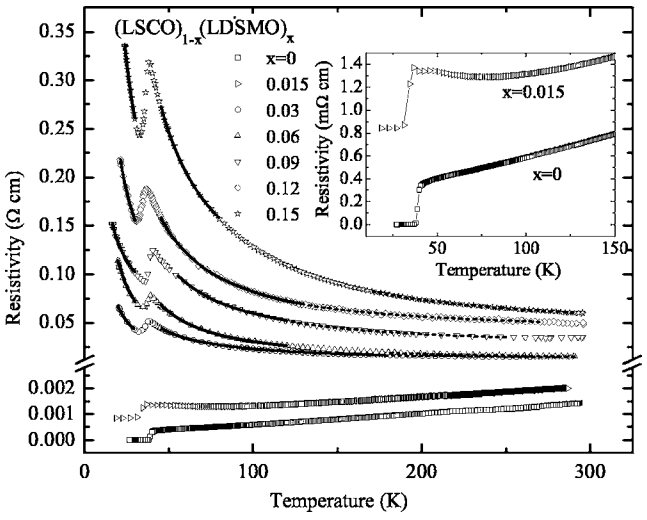

FIG. 5. Variation of the scaled (see the text) resistivity of LSCO and the composites with respect to temperature. The continuous lines are a fit to the resistivity assuming variable range hopping conduction below $\sim$120 K and the dashed lines represent a fit assuming thermally activated conduction above $\sim$180 K. The region near the superconducting transition of LSCO is shown in the inset for $x=0$ and 0.015.

In order to obtain better clarity for the observed changes in electrical properties of the composites we have tried to analyze the normal state resistivity considering different possible mechanisms for the origin of resistivity. An analysis using the variable range hopping (VRH) mechanism seems to explain the observed temperature dependence of resistivity reasonably well. The continuous lines in Fig. 5 represent the fit using the VRH formula, $R \sim a \times \sqrt{T} \exp(b/T^{0.25})$ for the composites. As can be seen from the figure, the data below $\sim$120 K can be fitted quite well with the above equation. This implies that the electrons are getting localized in the composites, and the conduction at low temperatures is essentially due to hopping of the electrons from one localized site to another. On the other hand, the resistivity data above $\sim$180 K of all the composites can be fitted to the formula $R \sim a' \times \exp(b'/T)$ that represents thermally activated conduction. The dotted lines in Fig. 5 represent the fitted curves using the above equation. The analysis shows that a simple variable range hopping mechanism is adequate to describe the temperature dependence of the composites with $x \geqslant 0.03$ at low temperatures. One of the possible reasons for such a change in the resistivity behavior can be that the intercalation of LDSMO may be leading to an electronic phase separation in LSCO with hole rich and hole poor regions. If that is the case the observed decrease in the superconducting volume fraction can be explained to be due to the absence of superconductivity in the hole poor regions of LSCO. More detailed microscopic measurements are required to verify this scenario.

Magnetization measurements were carried out at 10 K for all the samples as a function of applied field, the results of which are shown in Fig. 6. There is a monotonic increase in the saturation magnetization (M_s) with increase in x, and the value of M_s roughly scales with x, the LDSMO content in the composites, which is shown in the inset of Fig. 6; but the M_s of the composites does not scale with the bulk LDSMO magnetization value (last point corresponding to $x=1$ in the inset of Fig. 6) and are found to be slightly lower. We believe that the M_s of LDSMO in the composites becomes smaller com-

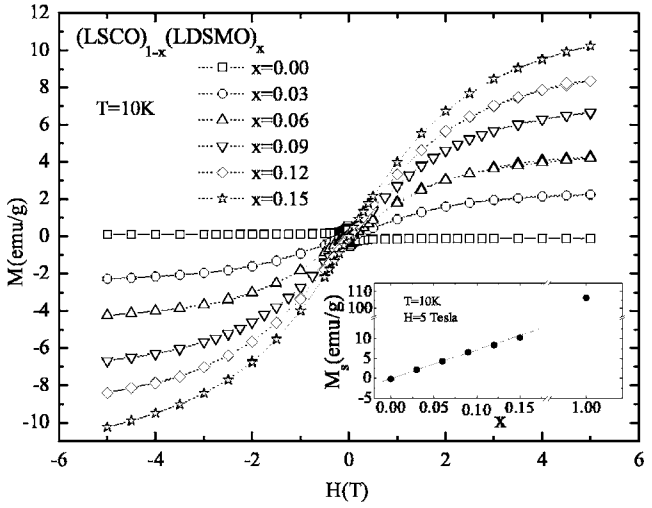

FIG. 6. Magnetization curves as a function of the applied field, measured at 10 K for the undoped LSCO and the composites. The saturation magnetization as a function of x is shown in the inset.

pared to the bulk value due to its smaller particle size in the composites as is evident from the SEM pictures. This kind of a decrease in the saturation magnetization with decrease in particle size has already been reported[25] in literature and has been attributed to the surface effects like vacancies, stress, etc. The increase in the saturation magnetization of the composites with x does not seem to affect the T_c of LSCO. However, the results of ac susceptibility and magnetization measurements as functions of temperatures are consistent with the resistivity data. Figure 7 represents the variation in dc magnetization (under zero field cooled and field cooled conditions) as a function of temperature, measured under an external dc field of 50 Oe, for the undoped LSCO as well as the composites. Temperature is plotted on a logarithmic scale so that the superconducting transition corresponding to LSCO and the magnetic transition of LDSMO can be clearly seen.

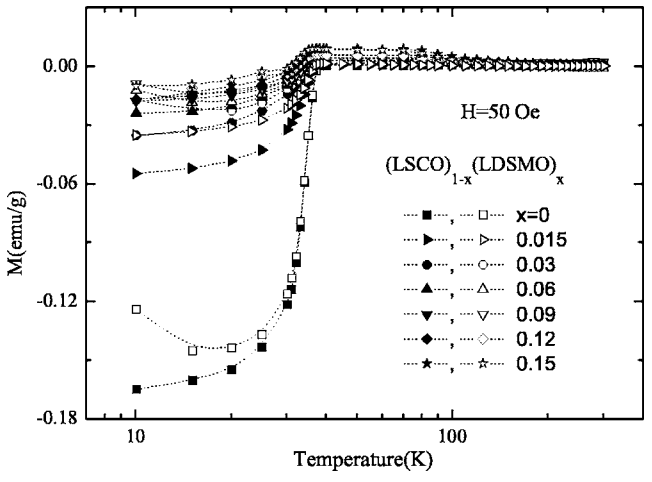

FIG. 7. Zero field cooled (closed symbols) and field cooled (open symbols) magnetization curves of the undoped LSCO and the composites with respect to temperature. Superconducting volume fraction decreases drastically on intercalation with LDSMO whereas T_c is almost unaffected.

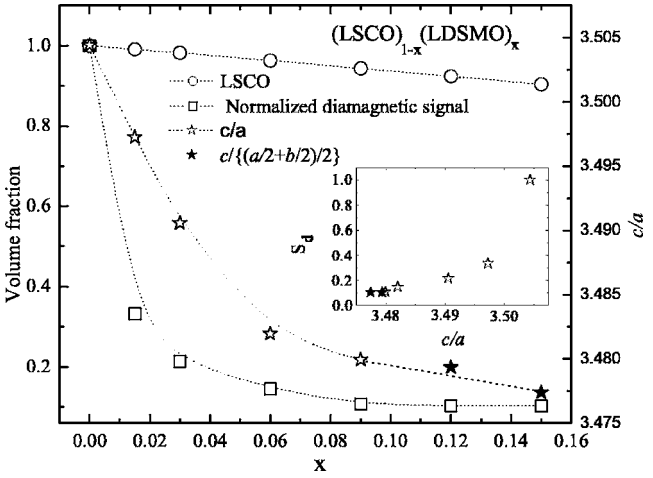

FIG. 8. Normalized diamagnetic signal (S_d), the actual volume fraction of LSCO in the composites, and the c/a ratio as a function of x. The variation of S_d as a function of c/a is shown in the inset. An almost linear dependence of S_d on c/a is observed for $x \geqslant 0.015$.

It can be seen from the figure that there is a drastic reduction in the superconducting volume fraction whereas the T_c is almost unaffected upon intercalation with LDSMO consistent with the resistivity data.

The normalized diamagnetic signal, which represents the superconducting volume fraction (with the value of LSCO to be normalized to 1), and the actual volume fraction of LSCO in the composites along with the variation in c/a ratio obtained from XRD analysis is shown in Fig. 8. The variation in superconducting volume fraction does not follow the actual volume of LSCO used in the composites. The decrease in superconducting volume fraction is drastic for small quantities of LDSMO intercalation. There is only a marginal decrease in the superconducting volume fraction when x is increased beyond 0.06; but there seems to be a correlation between the variation in superconducting volume fraction and the variation in the c/a ratio with respect to x. Both the c/a ratio and the superconducting volume fraction decrease drastically for small quantities of LDSMO whereas there is a tendency for saturation for larger LDSMO intercalation. If we take $c/[(a/2+b/2)/2]$ for $x=0.12$ and 0.15 (which show a doubling of the cell parameters, a and b), they will also fall in line with the figure of c/a vs x. These points are shown by filled stars in the figure. The variation of the normalized diamagnetic signal as a function of c/a is shown in the inset of Fig. 8 which shows an almost linear dependence for $x \geqslant 0.015$. These results, in comparison with the monotonic increase in saturation magnetization with x (inset of Fig. 6), implies that the short range ordering in LDSMO does not influence the superconductivity significantly, at least for the higher values of x. One of the reasons for the insignificant effect of the short range order of LDSMO may be the larger grain size of LSCO in comparison to the spin diffusion lengths. The characteristic spin diffusion length and ferromagnetic coherence length in the case of ferromagnet/superconductor heterostructures are in the nanometer range[26] and it will be much smaller in the case of LDSMO due to its

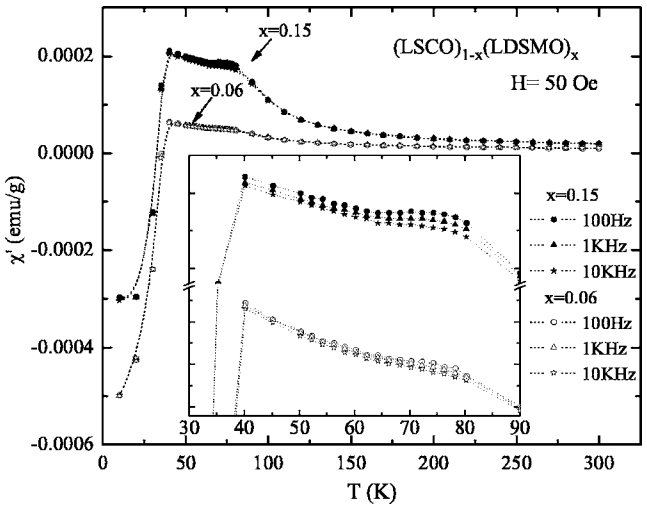

FIG. 9. Frequency dependent ac susceptibility as a function of temperature for the composites with $x=0.06$ and 0.15 is plotted. The region near the magnetic transition is expanded and is shown in the inset.

spin glass type order. The grain size of LSCO is much higher (of the order of a few microns) compared to this length scale.

The magnetic transition of LDSMO is also clearly seen in all the composites. An unusual increase in susceptibility is observed when the temperature is decreased below T_f. Such an increase in ac susceptibility, below T_f, is not present in undoped LDSMO.

In order to study the magnetic transitions more clearly, frequency dependent ac susceptibility measurements were done on all the composites. The measurements were carried out under an external dc field of 50 Oe. The results obtained for two representative composites with $x=0.06$ and 0.15 are shown in Fig. 9. A shoulder corresponding to the magnetic transition of LDSMO is observed at $T_f \sim 75$ K. The observed increase in T_f with increase in frequency clearly demonstrates the occurrence of spin glass transition in LDSMO.

The resistivity and magnetization measurements carried out on the composites suggest a transition of the metallic superconducting phase of LSCO to an insulating nonsuperconducting phase with the appearence of a weak magnetic phase, leading to an anomalous quenching of superconductivity for small concentrations of LDSMO. As mentioned in the Introduction the LSCO with the optimum Sr doping undergoes a spin glass transition[15] at very low temperatures ($\sim$45 mK). In addition, there are reports on the coexistence and competition between superconductivity and charge-stripe order in $La_{1.85-x}Nd_xSr_{0.15}CuO_4$ for $x=0.15$ and 0.20 from the neutron diffraction and zero field magnetization measurements by Tranquada *et al.*[27–29] They have proposed a static stripe correlation model in the low temperature tetragonal phase based on the superlattice peaks observed in neutron scattering experiments. The holes segregate to form a superlattice and the Cu spins in the hole-poor regions order antiferromagnetically below around 30 K. Our experimental results suggests that the intercalation of LDSMO gives rise to a distortion in the structure of LSCO, a metallic-to-insulating transition in resistivity and a partial quenching of superconductivity with the appearance of a weak magnetic transition. Based on our analysis, the origin of partial quenching of superconductivity in LSCO may be the distortion induced hole-segregation. The short range magnetic order of LDSMO is retained in the whole series of composites, with the saturation magnetization being proportional to the LDSMO content, which coexists with the superconductivity of LSCO.

IV. CONCLUSIONS

We have successfully synthesized the composites of $(La_{1.85}Sr_{0.15}CuO_4)_{1-x}(La_{0.3}Dy_{0.4}Sr_{0.3}MnO_3)_x$ for $x \leqslant 0.15$. The saturation magnetization increases monotonically with increase in x, indicating the gradual increase of the magnetic phase. The spin glass transition of LDSMO is clearly observed in the composites. Intercalation of small quantities of LDSMO in LSCO does not change the onset of superconducting transition temperature considerably; but, the superconducting volume fraction decreases drastically with increase in x. The metallic superconducting phase of LSCO changes to an insulating nonsuperconducting phase on intercalation with LDSMO. It is proposed that the intercalation induced structural distortion which leads to a hole segregation may be the cause for the observed metallic-to-insulating transition and the partial quenching of superconductivity. However, detailed microstructure analysis is required to confirm this point of view. The most unexpected results are the change from metallic to insulating-like behavior already at $x=0.015$ at low temperature and the quenching of LSCO superconductivity. Further work is needed to clarify this surprising result.

ACKNOWLEDGMENTS

This project was financially sponsored by National Science Council of R. O. C. under Grants No. 94-2120-M-002-011 and No. 94-2752-M-002-006-PAE.

*On leave from Materials Science Division, Indira Gandhi Centre for Atomic Research, Kalpakkam 603 102, India.
†Corresponding author. Email address: jglin@ccms.ntu.edu.tw

[1] B. Keimer, N. Belk, R. J. Birgeneau, A. Cassanho, C. Y. Chen, M. Greven, M. A. Kastner, A. Aharony, Y. Endoh, R. W. Erwin, and G. Shirane, Phys. Rev. B **46**, 14034 (1992).
[2] M. A. Kastner, R. J. Birgeneau, G. Shirane, and Y. Endoh, Rev. Mod. Phys. **70**, 897 (1998).
[3] M.-H Julien, Physica B **329-333**, 693 (2003).
[4] S. Uchida, Solid State Commun. **126**, 57 (2003).
[5] D. R. Harshman, G. Aeppli, G. P. Espinosa, A. S. Cooper, J. P. Remeika, E. J. Ansaldo, T. M. Riseman, D. Ll. Williams, D. R.

Noakes, B. Ellman, and T. F. Rosenbaum, Phys. Rev. B **38**, 852(R) (1988).
[6] F. C. Chou, F. Borsa, J. H. Cho, D. C. Johnston, A. Lascialfari, D. R. Torgeson, and J. Ziolo, Phys. Rev. Lett. **71**, 2323 (1993).
[7] F. C. Chou, N. R. Belk, M. A. Kastner, R. J. Birgeneau, and A. Aharony, Phys. Rev. Lett. **75**, 2204 (1995).
[8] S. Wakimoto, S. Ueki, Y. Endoh, and K. Yamada, Phys. Rev. B **62**, 3547 (2000).
[9] J. B. Torrance, Y. Tokura, A. I. Nazzal, A. Bezinge, T. C. Huang, and S. S. P. Parkin, Phys. Rev. Lett. **61**, 1127 (1988).
[10] T. Nagano, Y. Tomioka, Y. Nakayama, K. Kishio, and K. Kitazawa, Phys. Rev. B **48**, 9689 (1993).
[11] P. G. Radaelli, D. G. Hinks, A. W. Mitchell, B. A. Hunter, J. L. Wagner, B. Dabrowski, K. G. Vandervoort, H. K. Viswanathan, and J. D. Jorgensen, Phys. Rev. B **49**, 4163 (1994).
[12] K. Yamada, C. H. Lee, K. Kurahashi, J. Wada, S. Wakimoto, S. Ueki, H. Kimura, Y. Endoh, S. Hosoya, G. Shirane, R. J. Birgeneau, M. Greven, M. A. Kastner, and Y. J. Kim, Phys. Rev. B **57**, 6165 (1998).
[13] C. Panagopoulos, B. D. Rainford, J. R. Cooper, and C. A. Scott, Physica C **341-348**, 843 (2000).
[14] M.-H. Julien, A. Campana, A. Rigamonti, P. Carretta, F. Borsa, P. Kuhns, A. P. Reyes, W. G. Moulton, M. Horvatić, C. Berthier, A. Vietkin, and A. Revcolevschi, Phys. Rev. B **63**, 144508 (2001).
[15] C. Panagopoulos, J. L. Tallon, B. D. Rainford, T. Xiang, J. R. Cooper, and C. A. Scott, Phys. Rev. B **66**, 064501 (2002).
[16] C. Panagopoulos, J. L. Tallon, B. D. Rainford, J. R. Cooper, C. A. Scott, and T. Xiang, Solid State Commun. **126**, 47 (2003).
[17] C. Panagopoulos, A. P. Petrovic, A. D. Hillier, J. L. Tallon, C. A. Scott, and B. D. Rainford, Phys. Rev. B **69**, 144510 (2004).
[18] J. Olejniczak and A. J. Zaleski, Phys. Rev. B **54**, 80 (1996).
[19] V. A. Vas'ko, V. A. Larkin, P. A. Kraus, K. R. Nikolaev, D. E. Grupp, C. A. Nordman, and A. M. Goldman, Phys. Rev. Lett. **78**, 1134 (1997).
[20] V. Peña, Z. Sefrioui, D. Arias, C. Leon, J. Santamaria, J. L. Martinez, S. G. E. te Velthuis, and A. Hoffmann, Phys. Rev. Lett. **94**, 057002 (2005).
[21] P. Przyslupski, A. Tsarou, P. Dluzewski, W. Paszkowicz, R. Minikayev, K. Dybko, M. Sawicki, B. Dabrowski, and C. Kimaball, Supercond. Sci. Technol. **19**, S38 (2006).
[22] A.-M. Haghiri-Gosnet and J.-P. Renard, J. Phys. D **36**, R127 (2003).
[23] Daniel Hsu and J. G. Lin, J. Magn. Magn. Mater. **304**, e427 (2006).
[24] C. Mitra, P. Raychaudhari, S. K. Dhar, A. K. Nigam, R. Pinto, and S. M. Pattalwar, J. Magn. Magn. Mater. **192**, 130 (1999).
[25] M. A. López-Quintela, L. E. Hueso, J. Rivas, and F. Rivadulla, Nanotechnology **14**, 212 (2003).
[26] V. Peña, C. Visani, J. Garcia-Barriocanal, D. Arias, Z. Sefrioui, C. Leon, J. Santamaria, and C. A. Almasan, Phys. Rev. B **73**, 104513 (2006).
[27] J. M. Tranquada, B. J. Sternlieb, J. D. Axe, Y. Nakamura, and S. Uchida, Nature (London) **375**, 561 (1995).
[28] J. M. Tranquada, J. D. Axe, N. Ichikawa, Y. Nakamura, S. Uchida, and B. Nachumi, Phys. Rev. B **54**, 7489 (1996).
[29] J. M. Tranquada, J. D. Axe, N. Ichikawa, A. R. Moodenbaugh, Y. Nakamura, and S. Uchida, Phys. Rev. Lett. **78**, 338 (1997).